www.rericjournal.ait.ac.th

Floating PV Systems with Single-Axis Solar Tracking

Paweetida Chaiyapong*, Chutima Prasartkaew^, and Boonrit Prasartkaew*,[1]

ARTICLE INFO

Article history:
Received 06 May 2025
Received in revised form
09 August 2025
Accepted 29 August 2025

Keywords:
Floating photovoltaic (FPV)
Single-axis solar tracking
Solar energy optimization
Renewable energy systems
Performance analysis

ABSTRACT

The energy efficiency of a floating photovoltaic (FPV) system with a single azimuth-axis sun tracking mechanism is examined in this work. Installing FPV systems over water surfaces has several advantages, including easier rotation along a vertical axis, land conservation, and increased energy efficiency because of the water's natural cooling effect. Floating PV with Single-Axis Tracking (FPVSAT) is a novel feature of simple tracking for FPV that was proposed in this study. Since most conventional horizontal-axis tracking systems revolve around the horizontal N-S axis, single-axis trackers that spin around the vertical axis are somewhat unusual. The PV panels can follow the sun's azimuthal direction all day long the vertical-axis tracking design, which maximizes solar energy capture while preserving mechanical simplicity appropriate for floating buildings. Using experimental data from a prototype installed in Lop Buri, Thailand, a mathematical model was created and verified. We compared fixed, linear tracking, and vertical-axis azimuth tracking setups using simulations with high-resolution meteorological data. The azimuth tracking arrangement produces the maximum energy production, according to the results, highlighting the promise of vertical-axis tracking FPV systems as an affordable and scalable substitute for optimizing solar energy generation, especially in tropical areas with fluctuating sun patterns.

1. INTRODUCTION

Increasing demand for energy globally due to urbanization, population expansion, and technological innovation has highlighted the urgent need for healthier, more sustainable energy sources. Concurrently, concerns on climate change and the depletion of fossil fuel supplies have led to a boost in research and investment in renewable energy technologies [1], [2], and [3].

Among all renewable energy sources, solar energy is the most attractive because of its accessibility, adaptability, and low environmental effect [4], [5]. Photovoltaic (PV) systems are becoming more and more popular since the cost per kW and efficiency are getting better. They are soon becoming an important technology for turning sunlight into electricity [6], [7].

PV has demonstrated its capacity to reduce energy dependence on fossil fuels and contribute to climate objectives in both centralized infrastructures and off-grid applications [8]. However, the lack of available low-cost space is a main problem for placing up PV systems, especially in places with a lot of people. In order to resolve this issue, Floating Photovoltaic (FPV) systems have been developed, which employ the surface of reservoirs, lakes, and ponds to implement PV arrays. FPV systems provide a variety of benefits, including the reduction of land use conflict, the improvement of cooling for PV modules through the water surface, and the reduction of water runoff from reservoirs [9], [10], [11]. Because of these features, FPV is especially suitable for tropical areas with plenty of water bodies and strong sun irradiation, like Thailand [12].

To make a big difference in how much energy they make, PV and FPV systems are using more and more sun tracking algorithms. These systems follow the sun's motion across the sky so that panels may get the most sunlight. Dual-axis systems are frequently costly and hard to understand, but they do give the best alignment [13], [14]. Single-axis tracking, which until recently has a horizontal axis configuration [15] –[17], offers a better compromise between structural simplicity and efficiency gain.

FPV systems that use tracking face unique challenges, even when they work well. When buoyant platforms and moveable parts are put together, they can cause problems such system instability, corrosion, and trouble anchoring. Also, structural integrity requires taking into account environmental elements as wind and

---

https://doi.org/10.64289/iej.25.0309.2892571

* Department of Mechanical Engineering, Faculty of Engineering, Rajamangala University of Technology Thanyaburi, Thanyaburi, Pathum Thani, 12110, Thailand.

^ Department of Mathematics and Computer Science, Faculty of Science and Technology, Rajamangala University of Technology Thanyaburi, Thanyaburi, Pathum Thani, 12110, Thailand.

[1] Corresponding author:
Tel: +66 2 549 3430; Fax: +66 2 549 3433.
Email: boonrit.p@en.rmutt.ac.th

wave motion [18], [19]. The real-world adoption of these engineering challenges has been restricted, despite the fact that simulations and small-scale demonstrations continue to demonstrate significant performance benefits [20], [21].

Numerous researchers have investigated a variety of FPV systems, such as the longevity of the system, the cooling impacts on panels [22], [23], and the design considerations [24]. The potential for hybrid integration with PV systems has been demonstrated through the exploration of innovations such as the use of porous media in solar receivers to enhance thermal efficiency in water heating applications [25]. The potential for performance enhancement through innovative design and modeling is underscored by these interdisciplinary advancements.

Based on this background, the current work suggests and tests a Floating Photovoltaic system with a Single-Axis Tracking (FPVSAT) mechanism that spins around a vertical azimuth axis. This design is made for floating platforms, which makes it different from regular land-based N–S horizontal axis trackers. It is simple to use, affordable, and works well with water surfaces. We built and tested a whole mathematical model using real operational data from a prototype that was put up in Lop Buri, Thailand, and high-resolution meteorological information. The research looks at three different setups—fixed inclination, linear tracking, and azimuth tracking—under the same weather and geographic conditions to see how useful the suggested method would be in real life. This paper fills in a big gap in research by showing how an affordable, scalable tracking solution might improve the performance of FPV systems, especially in tropical and subtropical areas where there is a lot of solar potential and rivalry for land usage.

To addressing the research gap, this study aims to demonstrate how a scalable and affordable FPV system with single-axis tracking may increase energy output, particularly in tropical and subtropical locations. It is expected that the findings would influence future FPV system design in Southeast Asia and other regions with abundant sunlight.

2. MATERIALS AND METHODS

The design and operation of the proposed FPVSAT are described in this section. It demonstrates the new configuration of the system and its potential applications. With a focus on Thailand's solar energy potential and floating PV systems, the section also discusses the geographic and meteorological data used for the study.

2.1 Experimental Set-up

As shown in Figure 1, the main part of the proposed FPVSAT system is a collection of slanted PV panels installed on a floating platform with a sun-tracking device. From a sun-tracking perspective, the floating PV system's capacity to spin with little force is a key benefit. The system may be extended into massive arrays of PV panels because to this feature, which makes it extremely scalable.

Due to its very low rate of rotation, which is approximately 0.25 degrees per minute, the proposed FPVSAT system utilizes less energy. This slow speed allows for the operation of a low-power drive motor, a small cable, and a low energy consumption. In order to guarantee consistent sun-tracking performance and stability, the vertical pivot axis of the device can be fastened to either a conventional anchor or a ground-mounted underwater column. The proposed floating PV system is a viable and innovative option for large-scale solar energy applications due to its architecture, which emphasizes energy efficiency and scalability.

The operation of the proposed FPVSAT involves rotating it by using a speed adjustable electric gear-motor with two cable pulleys, as a cable winch. For clockwise rotation, it pulls a cable wound around pulley ‘b’ and, at the same time, the cable on another side will be released by pulley ‘a’, as shown in Figure 1. These cables are connected to points set with moving pulleys around the pond bank and their ends are attached to a fixed point on the opposite-side of float. The electricity generated by the PV can be distributed on ground via an underwater cable.

The float's operation begins at 6:00 a.m., facing east, and rotates southward toward the west. From 6:00 a.m. to 6:00 p.m. (180 degree), the floating PV must be rotated for 12 hours. At night, the float rotates back to its original position (done by converting the rotating direction of motor), ready to start for the next day.

2.2 Site Location

Thailand is a good place for solar energy since it is close to the equator, which means it gets a lot of sunlight all year round. The country is a great place for solar energy projects since it gets five to six hours of direct sunlight every day. Floating solar arrays atop reservoirs are also being looked into more and more as a way to make the most use of land and energy. Floating solar arrays work best in Thailand's deep-water reservoirs, which include lakes, dams, and big ponds.

2.3 Instrumentation and Data Acquisition

The instrumentation and data acquisition (DAQ) system were setup to enable accurate tracking monitoring and recording of solar radiation and also used for controlling the FPVSAT system. The following important components comprise in the experimental setup:

Two pyranometers were used to measure the amount of solar radiation. The tracking system's actual solar radiation was recorded by mounting one directly on the floating PV panel, aligned with the same inclination angle as the panel. Another pyranometer was installed on land with an inclination angle that corresponded to the latitude of the site and was also oriented directly south. This functioned as a reference measurement for fixed systems and facilitated the validation of the simulation model.

There is a control box on ground where DAQ system with a data logger and controller are installed inside. It continuously recorded signals from both pyranometers and saved the data for further processing and using for the developed model validation. Inside this small room, charging controller, dummy loads, and other electronics that used for power management and safety are stored. Some of these could be used later in the future study.

The floating platform was rotated by a gear motor with an adjustable speed rate. The speed and rotation direction of the motor was controlled using a programmable control unit. The floating building was pulled along a steel cable that wound around cable pulleys that were thoughtfully positioned on the pond shore by a cable winch that was activated by the motor. At a rate of around 0.25 degrees per minute, this configuration allowed the platform to spin smoothly around the azimuth.

In order to prevent low energy loss and preserve the stability of the floating system, the electricity generated by the floating PV panels was transferred to the onshore system via an underwater cable. Furthermore, the signal from the later pyranometer was wired via same underwater connection.

Instrumentation was installed to cope with outside conditions and thoughtfully aligned to ensure accuracy. Data was collected under clear skies at 30-minute intervals throughout the day to support both real-time monitoring and model validation activities.

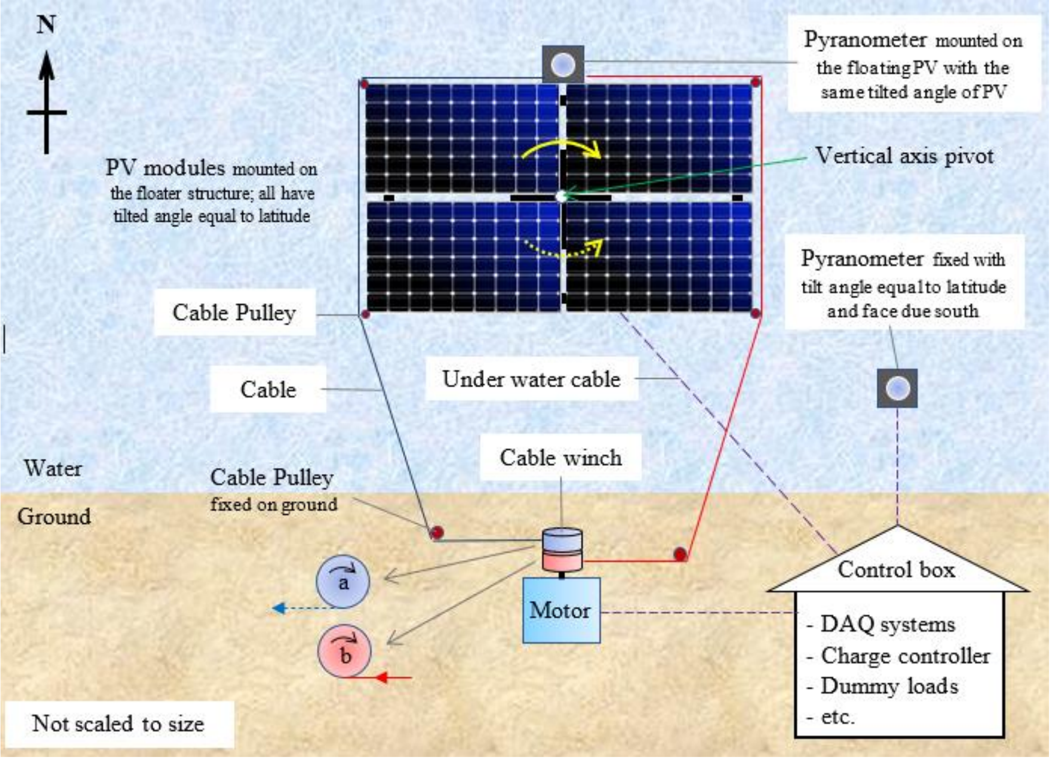

Fig. 1. Proposed floating PV and sun tracking mechanism.

2.4 *Weather Input Data*

This research looks at how well and how possible it is to establish a real floating photovoltaic system with single-axis solar tracking at an FPV facility in latitude 14°02'01"N and longitude 100°43'31"E. We used five-minute weather data from the Asian Institute of Technology's meteorological station in Bangkok, Thailand, to build the system and test how it would work.

The results of this investigation will indicate whether the proposed FPVSAT technology is a viable and sustainable alternative to conventional land-based photovoltaic systems in Thailand. It also provides a comprehensive assessment of the system's efficacy by incorporating a significant amount of local meteorological data.

3. MATHEMATICAL MODEL AND VALIDATION

Factors such as the Earth's axial inclination, geographical latitude, day duration, and local weather conditions, which can vary significantly by season and location, are all critical to the availability of solar energy. Regionally, solar energy is more consistent in regions that are closer to the equator, while areas at higher latitudes experience more seasonal variation. The Earth's inclination leads to fluctuations in the duration of the day and the angle of sunlight, which results in longer, sunnier days during the summer and shorter, less intense days during the winter. Local meteorological factors that may influence the amount of sunlight that reaches the Earth's surface including humidity, pollution, and cloud cover. In order to get the greatest outcomes, these variations highlight the significance it is to adjust solar energy systems to the particular seasonal and geographic conditions. This is achieved by developing a mathematical model to conduct feasibility studies.

This study aims to evaluate how the performance of a conventional floating PV system (fixed and south-facing) can be enhanced using the proposed single-axis sun-tracking method. To estimate the solar radiation incident on the tilted PV panel surface—serving as the input energy to be converted into electricity—the 'Isotropic Sky Model,' as referenced in [27], is employed in this analysis.

3.1 Equations

To simulate both fixed and rotating (moving) tilted surfaces, it is essential to calculate all fundamental sun-Earth relationship variables, weather conditions, as well as extraterrestrial and terrestrial solar insolation. These calculations rely on input parameters, which include location-specific and weather condition data, as outlined below.

- the date and watch time
- the latitude angle ($\emptyset$) of site location
- the tilted angle of PV-panel (β)
- the azimuth angle of PV-panel (γ)
- the typical annual daily terrestrial radiation (H in MJ/m^2) (may using the typical meteorological year (TMY) of the site location.

Calculating the declination (δ) as:

$$\delta = 23.45\ \sin[360(284 + \mathrm{N})/365 \tag{1}$$

where, N is the day number of the year.

Calculating the solar time (ST) as:

$$\mathrm{ST} = \mathrm{WT} + \mathrm{EOT} - \Delta \tag{2}$$

where, WT is watch time.

EOT is equation of time can be calculated, in minute, as:

$$\mathrm{EOT} = 9.87 \sin 2\mathrm{B} - 7053 \cos \mathrm{B}) - 1.5 \tag{3}$$

where;

$$\mathrm{B} = 360(\mathrm{N} - 81)/364 \tag{4}$$

where, N is the day number of the year, Δ is time correction factor or longitude correction (in minute) can be calculated using the local standard time meridian or longitude (L_{st}) and local longitude (L_{lo}) as:

$$\Delta = 4\ (\mathrm{L_{st}} - \mathrm{L_{lo}}) \tag{5}$$

where;

$$L_{st} = 15(\Delta_{GMT}) \tag{6}$$

Calculating the hour angle as:

$$\omega = 15(\mathrm{ST} - 12) \tag{7}$$

where, ST is solar time in hours (*e.g.*: 10:30 = 10.5 hr or 10:45 = 10.75 hr).

Calculating the radiation falling on the tilted PV-panel surface (I_T in MJ/m^2) using as:

$$\mathrm{I_T} = \mathrm{I_b R_b} + \mathrm{I_d}\frac{(1 + \cos\beta)}{2} + \mathrm{I}\rho\frac{(1 - \cos\beta)}{2} \tag{8}$$

where, ρ is a constant ground reflectance or albedo of various surfaces (the value used in this study is 0.2). I_b is beam radiation from the sun equal to:

$$\mathrm{I_b} = \mathrm{I} - \mathrm{I_d} \tag{9}$$

where, I is global radiation from the sun can be calculated as:

$$\mathrm{I} = \left[\frac{\pi}{24}(\mathrm{a} + \mathrm{b}\ \cos\omega)\frac{\cos\omega - \cos\omega_s}{\sin\omega_s - \frac{\pi}{180}\omega_s\cos\omega_s}\right]\mathrm{H} \tag{10}$$

where, $\mathrm{a} = 0.409 + 0.5016 \sin(\omega_s - 60)$
$\mathrm{b} = 0.6609 - 0.4767 \sin(\omega_s - 60)$

and the sunrise or sunset hour angle, (ω_s) is calculated from:

$$\cos\omega_s = -\tan\delta\tan\emptyset \tag{11}$$

where, I_d is diffuse radiation from the sky can be calculated as:

$$\mathrm{I_d} = \left[\frac{\pi}{24}\frac{\cos\omega - \cos\omega_s}{\sin\omega_s - \frac{\pi}{180}\omega_s\cos\omega_s}\right]\mathrm{H_d} \tag{12}$$

where, H_d is daily horizontal diffuse radiation can be calculated as:

For the case that $\omega_s \leq 81.4°$,
For $K < 0.715$,

$$\mathrm{H_d} = \begin{bmatrix}1.0 - 0.2727\mathrm{K} + 2.4495\mathrm{K}^2 \\ -11.9514\mathrm{K}^3 + 9.3879\mathrm{K}^4\end{bmatrix}\mathrm{H} \tag{13}$$

otherwise,

$$\mathrm{H_d} = 0.143\mathrm{H} \tag{14}$$

For the case that $\omega_s > 81.4°$,
For $K < 0.722$,

$$\mathrm{H_d} = \begin{bmatrix}1.0 + 0.283\mathrm{K} - 2.5557\mathrm{K}^2 \\ +0.8448\mathrm{K}^3\end{bmatrix}\mathrm{H} \tag{15}$$

otherwise,

$$\mathrm{H_d} = 0.175\mathrm{H} \tag{16}$$

where, the daily clearness index (K) can be estimated from:

$$\mathrm{K} = \frac{\mathrm{H}}{\mathrm{H_0}} \tag{17}$$

where, the intensity of extraterrestrial radiation falling on a horizontal surface (H_0 in J/m^2) can be estimated from:

$$\begin{aligned}\mathrm{H_0} = \left[\frac{24 \times 3600}{\pi}\right]\mathrm{I_{sc}}[1 + 0.033\cos\frac{360\mathrm{N}}{365} \\ [\cos\emptyset\cos\delta\sin\omega_s + \frac{\pi}{180}\omega_s\sin\emptyset\sin\delta]\end{aligned} \tag{18}$$

where, the value of solar constant (I_{sc}) is 1,367 W/m^2.

The geometric factor (R_b), the ratio of the beam radiation on tilted surface to that on a horizontal surface at any time can be calculated as:

$$\mathrm{R_b} = \cos\theta\ /\ \cos\theta_z \tag{19}$$

where, the cosine of incidence angle (θ) and zenith angle (θ_z) can be calculated as

$$\begin{aligned}\cos\theta = {} & \sin\delta\sin\emptyset\cos\beta \\ & - \sin\delta\cos\emptyset\sin\beta\cos\gamma \\ & + \cos\delta\cos\emptyset\cos\beta\cos\omega\end{aligned} \tag{20}$$

$$+\cos\delta\sin\emptyset\sin\beta\cos\gamma\cos\omega + \cos\delta\sin\beta\sin\gamma\sin\omega$$

$$\cos\theta_z = \sin\emptyset\sin\delta + \cos\emptyset\cos\delta\cos\omega \quad (21)$$

In this study, all the aforementioned equations are systematically solved and analyzed using Microsoft Excel, following the same approach as in [28] with different equations.

4. ASSUMPTIONS USED IN THIS STUDY

The "Isotropic Sky Model" makes various assumptions about how solar radiation hits a slanted surface that make it easier to look at the three kinds of radiation (diffuse, direct, and reflected). The following are the assumptions that make up these:

1. Uniform Diffuse Radiation: The model suggests that the strength of diffuse radiation from the sky doesn't alter based on where the sun is since it travels the same way in all directions. Normally, the sky is lighter near the sun, but this approach doesn't take that into consideration.
2. There is no circumsolar effect since the model does not take into account circumsolar radiation, which is the brightening that happens around the sun's disk. People think that dispersed radiation is spread out equally throughout the sky dome.
3. The albedo value was chosen to 0.20 since the FPVSAT system was tested in a small pond near to dirt and concrete-covered ground. The ground-reflected irradiance was higher than the water's because the PV panels were largely facing the pond bank. The value picked was more accurate than the true conditions, even though water usually has an albedo of 0.06. When simulating systems in open water bodies, a lower albedo should be employed to get more accurate results.
4. No Shading Effects: The model assumes that there are no trees, buildings, or other objects nearby that may block some of the direct or diffuse radiation.
5. Fixed Tilt Angle and height: It is assumed that the tilt angle and height of the surface stay the same for each calculation step, even if small changes might happen because of problems with the mounting or changes in the tracking systems.
6. Perfect Weather Conditions: The direct radiation part depends on the atmosphere being fixed in perfect weather conditions. These variations in temperature, dust, and air mass are very transitory, therefore they may not have a big influence on radiation levels.
7. The solar location, including its direction and altitude, maintains the same during each time step of the activity. The angles of the sun fluctuate over the day, but this makes it easy to calculate out the impact angles.

To make sophisticated radiation models easier to grasp, we have to make some assumptions. However, they may not be exactly how things are in the real world.

5. MODEL VALIDATIONS

Experimental findings from a genuine FPVSAT prototype were used in a validation procedure to evaluate the correctness of the established mathematical model (as shown in Figure 2). With a standard meridian longitude (L_{st}) of 105°E, the prototype was tested in Mueang District, Lop Buri, Thailand, which is situated at latitude 14°46'47"N, local longitude 100°42'28"E.

The model was fed all of the experimental system's parameters as input data. The simulation results were compared with the observed solar insolation incident on the PV panel surface on a day with clear skies for validation.

Solar insolation was measured and recorded using a data recorder that collected data from pyranometers positioned on the FPVSAT platform and another pyranometer positioned at the same level above the water's surface. The data logger was programmed to record values at 30-minute intervals, allowing for a detailed analysis of the system's performance under real-world settings.

By examining the measurement uncertainties, the reliability of the experimental findings was evaluated. Measurement uncertainty was estimated using the precision of the pyranometer utilized in the setup, as solar irradiance was directly recorded in W/m². The absolute uncertainty (ABU), as determined by the device specs, was 9.4%.

Two statistical measures, Root Mean Square Error (RMSE) and Mean Bias Difference (MBD), along with the measurement uncertainties mentioned in [28], were employed to evaluate and compare the experimental results with the model predictions.

The RMSE is calculated as follows:

$$RMSE = \sqrt{\frac{\sum_{i=1}^{N}(C_i - M_i)^2}{N}} \quad (22)$$

MBD can be calculated as:

$$MBD = \frac{1}{N}\sum_{i=1}^{N}(C_i - M_i) \quad (23)$$

where C_i represents the simulated values from the model, M_i denotes the corresponding measured values, and N is the total number of data points.

When the computed RMSE and MBD values are approximately equal to the measurement uncertainty, it suggests strong agreement between the model and the experimental data. Further details regarding model validation are provided in Section 6.1.

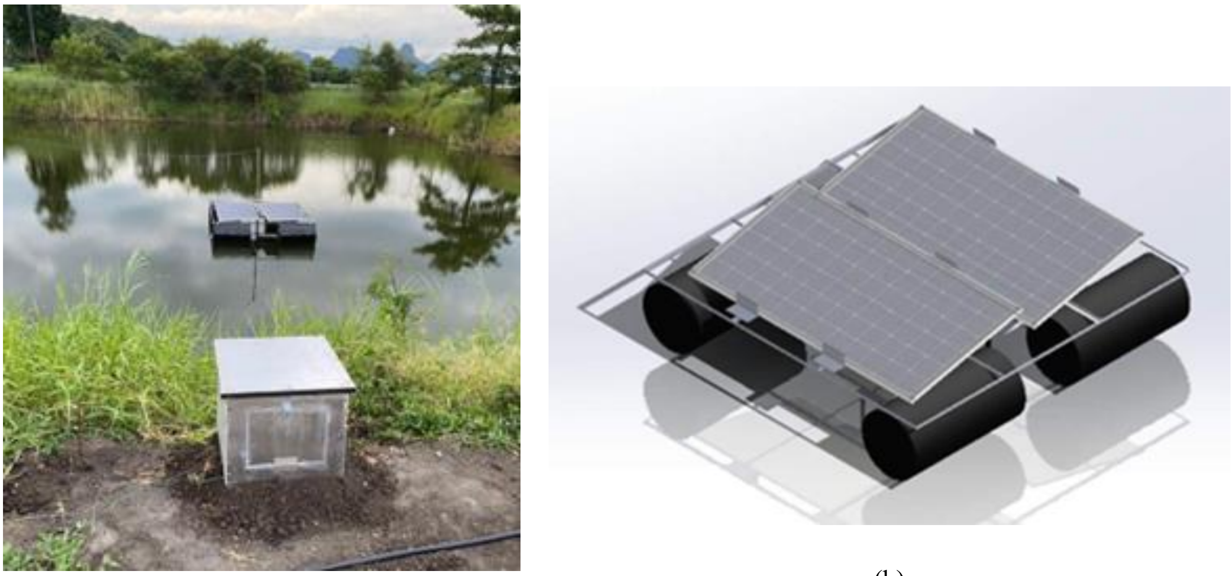

(a)

(b)

Fig. 2. A prototype floating PV used for model validation. (a) Experimental setup at the test site; (b) Drawing of FPVSAT used in this study.

6. RESULTS AND DISCUSSION

In this part of the theoretical research, we look at and compare how well an FPV system works in three different setups, which are shown below:

1. Fixed Configuration: In this configuration, the PV panels are placed on a solid floater and tilted at an angle that is right for the latitude. There is no such thing as sun-tracking technology.
2. Linear Tracking Configuration: The PV panels are mounted to a single floater and inclined to the latitude of the location. The whole system moves smoothly in a horizontal direction from -90° (east) to +90° (west).
3. Sun Azimuth Tracking Configuration: This setting rotates the PV panels in real time to keep them in line with the sun's azimuth angle once they have been tilted to the site latitude and set on a consolidated floater.

Floaters are easy to use and don't need much power to spin, which is a big plus. The linear tracking arrangement is not as good as the solar azimuth tracking setup, but it is easier and cheaper to use. This is why it's a good idea to implement it.

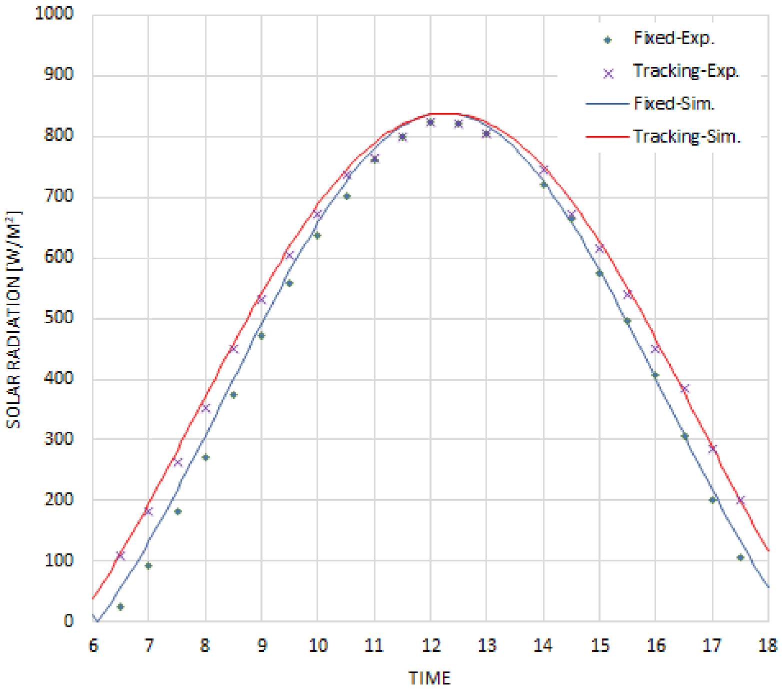

Fig. 3. Validation of the model through a comparison of simulation results with experimental data.

6.1 Validation Results

To validate the developed model, the results of the simulation were compared with the experimental results obtained from the experimental setup shown in Figure 2. A mention in [27], [28], the daytime from 6:00 AM to 6:00 PM should be focused. As mentioned in the assumption section, the experimental results of a very clear sky must be chosen and taken for model validation. Simulation results on the solar radiation profiles of two cases: fixed and single axis solar tracking, were compared with the measured values (May 1st, 2025) as shown in as shown in Figure 3.

To know the reliability of developed model, the results of observed experimental results were compared with the predicted results from the simulation. The calculated statistical parameters, RMSE and MBD, of all solar radiation are very close to the uncertainty of the measurements. The average value of RMSE and MBD were 9.6 and 9.5%, respectively. The results show that the simulation results are in good agreement with the experimental results.

6.2 Performance Analysis

To analyze the daily performance of the proposed FPVSAT, the mean day of the month mentioned in [27], as shown in Table 1, are used as input parameter.

Table 1. The mean day of the month.

Months	n for *i*th Day of Month	Mean Day of Month
January	i	17
February	31+i	16
March	59+i	16
April	90+i	15
May	120+i	15
June	151+i	11
July	181+i	17
August	212+i	16
September	243+i	15
October	273+i	15
November	304+i	14
December	334+i	10

The average day of the month is used as an input to see how well the proposed FPVSAT performs each day. The data in the appendix show how much solar radiation there is on an average day of each month. We will use the simulation result from July 17th as an example of how well the system performs every day. We speak about how the three instances are different: "Fixed" (blue line), "Linear tracking" (red line), and "as solar azimuth" (green line). The results show that both tracking methods ("Linear tracking" and "as solar azimuth") work better than the fixed system in the morning (6:00–8:00 AM) and late in the afternoon (4:00–6:00 PM). The "as solar azimuth" setting provides a little advantage because it is more aligned with the sun's azimuth. Around noon, when solar energy is at its peak, it's harder to tell the difference between the three systems.

The "as solar azimuth" technique, on the other hand, is still better because it is more in line with the sun's angle. As expected, the stationary system obtains the least amount of solar energy during the day (3.86 kWh/m^2/day) since it can't move to follow the sun. The linear tracking system collects a lot more solar energy (4.18 kWh/m^2/day), especially in the middle of the morning and afternoon when it is lined up with the sun's position. This makes it more efficient than the fixed system. The green line illustrates the "as solar azimuth" option, which has the highest total solar radiation values (4.24 kWh/m^2/day), especially during the busiest hours. This method seems to work best for lining up with the sun's path, which means it gets the maximum solar energy.

Figure 4 shows how much solar energy strikes the earth on average every day over the course of a year. The stationary system always has the lowest daily incidence radiation all year round. It has a seasonal pattern (highest in winter and lowest on rainy days), but it can't alter with the sun's location, which makes it less efficient, especially when the sun is low in the sky. Linear tracking is a major improvement over the fixed system, especially in the summer when the days are longer. This is because it moves the screen to better match up with the sun. But it still doesn't work as well as the "as solar azimuth" method, especially in the summer when azimuth alignment makes it even better at capturing energy. This technique works better than the other two all year long because it can accurately follow the sun's azimuth angle. This maintains the daily radiation levels higher. The change is most obvious when the sun is high in the sky, which means it works better.

The fixed system gets 1.41 MWh/m^2/year from solar energy each year, whereas the linear tracking system gets 1.53 MWh/m^2/year, which is an 8.2% increase. The "as solar azimuth" system has the best yearly production at 1.55 MWh/m^2/year. This is a 9.8% improvement over the fixed system and a little 1.4% gain over the linear tracking system. Even if linear tracking has gotten a little better, the "as solar azimuth" technique is still the best way to get the most energy out of the sun.

6.3 Influences of Latitude on System Performance

To analyze the influences of location at any latitude angle on the performance of the proposed FPVSAT, the mean days of the month are used as input parameter. The variation of latitude angle from the equator to 60 (High Latitude) degrees is used for simulation. Figure 5 shows the Daily solar energy of all mean days over year at latitude angle of 0° (Equator), 14.78° (Tropical Zone), 30° (Subtropical Zone) and 45° (Temperate Zone). In addition, the simulation results of higher latitude are in the same trend.

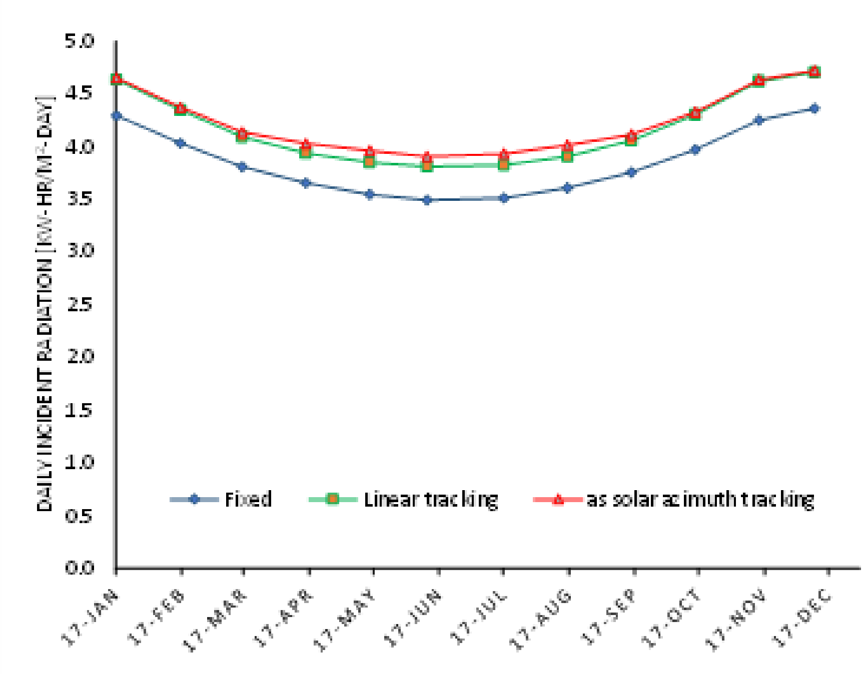

Fig. 4. Daily solar energy of all mean days over year at Ø = 14°46'47"N, L_{lo} = 100°42'28"E.

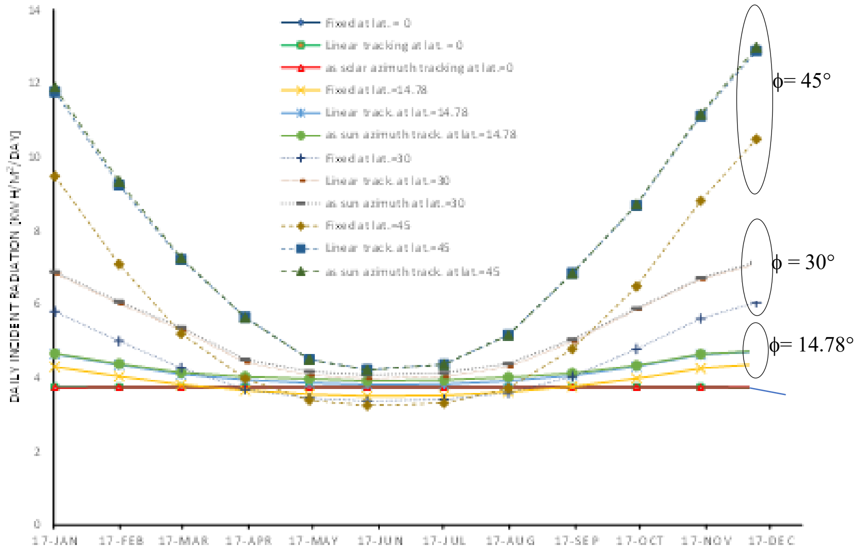

Fig. 5. Daily solar energy of all mean days over year at latitude angle of 0, 14.78, 30 and 45°.

As latitude increases from the equator to 60°, the overall daily incident solar radiation decreases for fixed solar panels but increases significantly for systems utilizing linear and azimuth tracking. Fixed systems show consistent but lower solar energy output across all latitudes. Linear tracking and azimuth tracking systems provide significantly higher energy yields, especially at higher latitudes. At higher latitudes (e.g., 45° and 60°), the seasonal variation in solar energy is much more pronounced compared to regions closer to the equator. At higher latitudes show lower energy outputs for fixed systems, whereas 'as sun azimuth tracking' systems maintain relatively higher performance, but very close to 'linear tracking' system.

Figure 6 shows the simulation results of the influences of latitude angle on the daily total radiation. At the Equator, the values of total radiation are consistent at 3.74 kWh/m²/day across fixed, linear, and azimuth tracking systems, with no significant improvement from tracking mechanisms. Mean that tracking systems do not provide any benefit at the equator due to the high and consistent solar angles throughout the year.

In the tropics, fixed systems make 3.86 kWh/m²/day. Linear tracking makes 4.18 kWh/m²/day (+8.21%), while azimuth tracking makes 4.24 kWh/m²/day (+9.75%). Tracking systems offer a tiny advantage, thus they can be utilized to make little energy benefits in tropical places where the seasons don't change much.

In the subtropical zone (around 30° of latitude), stationary systems obtain 4.42 kWh/m²/day of radiation. Linear tracking receives 5.29 kWh/m²/day, which is 19.79% more than before. Azimuth tracking gets 5.36

kWh/m²/day, which is 21.35% more. Tracking systems provide a lot of extra energy every year, which illustrates how valuable they are in subtropical places where the angle of the sun varies more over the year.

Fixed systems make 5.83 kWh/m²/day in the temperate zone, which is about 45° of latitude. This goes up to 7.63 kWh/m²/day (+31.02%) with linear tracking and 7.67 kWh/m²/day (+31.61%) with azimuth tracking. In temperate places where the seasons fluctuate a lot, tracking systems are much better than fixed systems.

For places with high latitudes, fixed systems yield 13.00 kWh/m²/day. Linear tracking offers 17.42 kWh/m²/day, which is 34.02% more than before. Azimuth tracking gives 17.40 kWh/m²/day, which is 33.91% more than before. Tracking systems have come a long way, and they are now critical to keep energy production running in locations with major seasonal fluctuations and low sun angles.

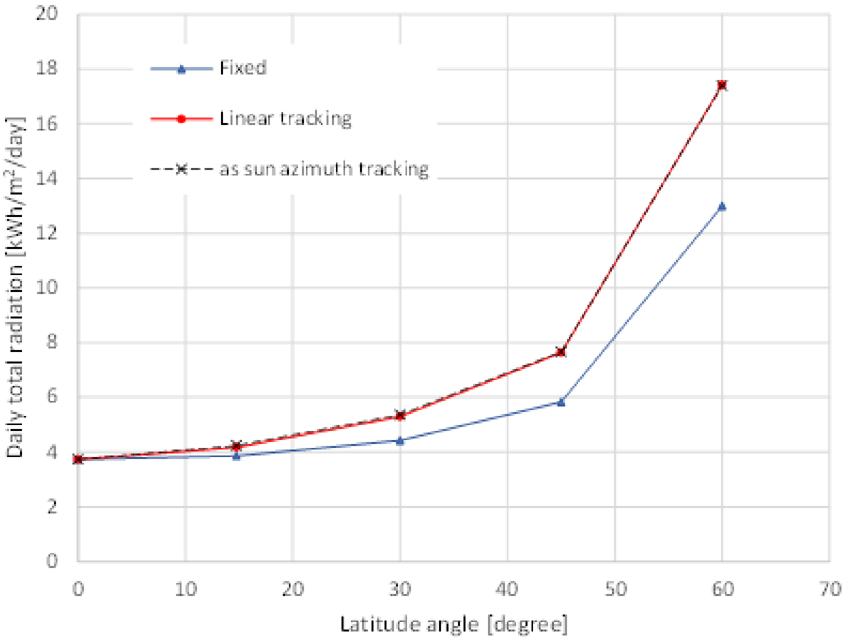

Fig. 6. Influences of latitude angle on the daily total radiation.

7. CONCLUSIONS

This study shows how important location and methods for tracking the sun are for making solar energy systems work better. The results show that fixed systems FPV work best in areas with a latitude of 0°, where the weather doesn't change much with the seasons and the sun is always shining. They are a good choice for projects that need to stay within a budget because they use a steady but limited amount of energy. Single-axis sun-tracking systems improve solar energy by 9.75% per year on average, which is a lot more than fixed systems. Tracking along sun direction systems is the best way to get the most energy returns in tropical and high-latitude areas (30° to 60°). There is a good mix between energy output and system complexity in linear tracking systems, which is why they are less expensive than azimuth tracking systems.

Higher areas have worse fixed systems because the sun's angle is lower and yearly changes are more noticeable. Solar tracking systems, especially azimuth tracking, help make sure that power is always reliable and efficient by taking care of these problems. In subtropical and tropical areas, where the sun's angles stay the same, fixed devices might be enough. Tracking devices are needed in high-latitude and warm areas to get the most out of solar energy and deal with changes that come with the seasons.

To get the most out of solar energy harvesting, you need to make smart investments in solar tracking systems and use designs that are made for your unique spot. Linear tracking systems are better for real-world use because they are more useful and cost less than azimuth tracking systems, even though they are not as good. This study shows how important it is to use solar energy systems that are tailored to local needs in order to get the most energy out of them and make sure they will last for a long time.

The method used in this study gets around a few practical problems by making the tracking device easier to use by rotating slowly and using little power. Most FPV tracking systems need complicated ways to keep them stable or attach them to something solid. The prototype, on the other hand, uses a cable-pulley system that is attached to the bank of the pond. This is easy to set up and doesn't cost too much for small ponds. Because of these features, it might be easier for people to use in real life.

ACKNOWLEDGEMENTS

The authors would like to express their gratitude to Rajamangala University of Technology Thanyaburi

(RMUTT) for financial support of this research publication.

REFERENCES

[1] Prasartkaew B. and A. Ngernplabpla. 2014. Investigation on the performance of a paraboloids heliostat for concentrated central receiver solar collector. In *Proc. 6th Int. Conf. on Science, Technology and Innovation for Sustainable Well-Being (STISWB VI)*: Siem Reap, Cambodia.

[2] Prasartkaew B. and S. Sukpancharoen. 2021. An experimental investigation on a novel direct-fired porous boiler for low-pressure steam applications. *Case Studies in Thermal Engineering* 26: 101-169.

[3] International Energy Agency, 2021. *World Energy Outlook 2021*, Paris: IEA Publications.

[4] Prasartkaew B. and S. Kumar. 2014. Design of a renewable energy based air-conditioning system. *Energy and Building* 68: 156–164.

[5] Prasartkaew B., 2018. Efficiency improvement of a concentrated solar receiver for water heating system using porous medium. *IOP Conference Series: Materials Science and Engineering* 297: 012-059.

[6] United Nations Environment Programme, 2020. *Emissions Gap Report 2020*, UNEP Publications.

[7] Lewis N.S. and D.G. Nocera. 2006. Powering the planet: Chemical challenges in solar energy utilization. *Proceedings of the National Academy of Sciences USA* 103(43): 15729–15735.

[8] Fthenakis V.M., 2009. Sustainability of photovoltaics: The case for thin-film solar cells. *Renewable and Sustainable Energy Rev*iews 13(9): 2746–2750.

[9] Fraunhofer Institute for Solar Energy Systems, 2020. *Photovoltaics Report*: [Online] Available: https://www.ise.fraunhofer.de

[10] Intergovernmental Panel on Climate Change, 2018. *Global Warming of 1.5°C*: IPCC.

[11] Choi Y., Lee K., and Kim H., 2014. A study on power generation analysis of floating PV system considering environmental impact. *Environmental Science and Technology* 48(22): 13125–13132.

[12] Liu H., Wang Z., and He W., 2017. Evaluation of floating photovoltaic systems' cooling effect on photovoltaic panels. *Journal of Renewable Energy* 21(3): 319–328.

[13] Chatterjee S. and A. Chatterjee. 2019. Types and benefits of solar tracking systems in photovoltaic applications. *Renewable Energy Rep*orts 24(2): 45–54.

[14] Kacira M., 2016. Analysis of single-axis and dual-axis tracking PV systems: Efficiency and cost implications. *Solar Energy* 134: 14–23.

[15] Sanchez J. and F.J. Batlles. 2019. Performance analysis of single-axis tracking PV systems: A case study. *Energy Conversion and Management* 182: 46–58.

[16] Mizuno T., 2017. Performance improvements in floating solar plants with tracking mechanisms. *International Journal of Photovoltaic Systems* 6(4): 110–115.

[17] Choi J., Lee K., and Kim H., 2014. A study on power generation analysis of floating PV system considering environmental impact. *Environmental Science and Technology* 48(2): 13125–13132.

[18] Liu H., Wang Z., and He W., 2017. Evaluation of floating photovoltaic systems' cooling effect on photovoltaic panels. *Journal of Renewable Energy* 21(3): 319–328.

[19] Liu H.Z., Li C.T., and Zhang J.W., 2020. Environmental benefits of floating PV on artificial water bodies. *Energy Reports* 6: 1216–1222.

[20] Smith R. and L. Jones. 2019. Global adoption trends in floating photovoltaic systems. *International Journal of Renewable Energy* 23(1): 1–9.

[21] Mizuno T., 2017. Performance improvements in floating solar plants with tracking mechanisms. *International Journal of Photovoltaic Systems* 6(4): 110–115.

[22] Wang L., Zhao Q., and Zhou X., 2020. Challenges and advancements in tracking mechanisms for FPV systems. *IEEE Transactions in Sustainable Energy* 11(2): 486–493.

[23] Patel N. and P. Kumar. 2021. Comparative analysis of land-based and floating PV systems under varying environmental conditions. *Renewable Energy* 29(2): 204–210.

[24] Erbs D.G., Klein S.A., and Duffie J.A., 1982. An equivalent mean day calculation to predict monthly average daily utilizability for flat plate collectors. *Solar Energy* 28(6): 413–417.

[25] Prasartkaew B. and S. Kumar. 2013. Experimental study on the performance of a solar-biomass hybrid air-conditioning system. *Renewable Energy* 57: 86–93.

[26] Prasartkaew B. and S. Kumar. 2010. A low carbon cooling system using renewable energy resources and technologies. *Energy and Buildings* 42(9): 1453–1462.

[27] Duffie J.A., Beckman W.A., and Blair N., 2020. *Solar Engineering of Thermal Processes, Photovoltaics and Wind*: Wiley.

[28] Prasartkaew B., 2013. Mathematical modeling of an absorption chiller system energized by a hybrid thermal system: Model validation. *Energy Procedia* 34: 159–172.

APPENDIX

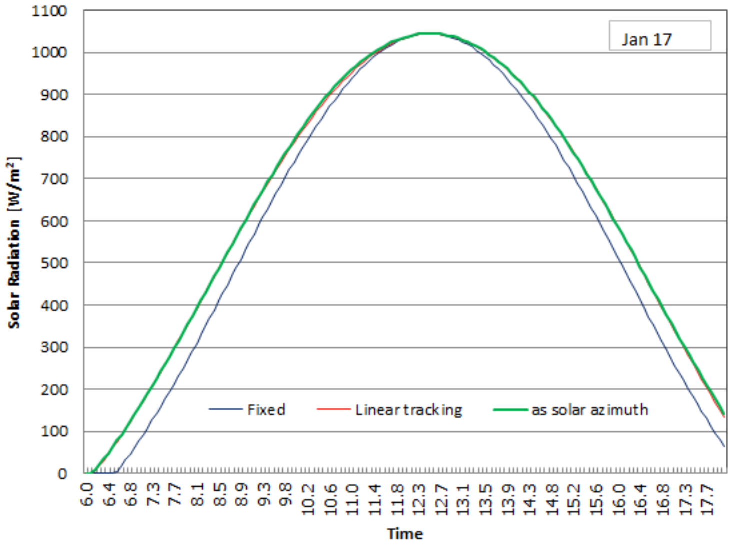
Jan 17
Solar Radiation [W/m²]
0
100
200
300
400
500
600
700
800
900
1000
1100
Fixed
Linear tracking
as solar azimuth
6.0
6.4
6.8
7.3
7.7
8.1
8.5
8.9
9.3
9.8
10.2
10.6
11.0
11.4
11.8
12.3
12.7
13.1
13.5
13.9
14.3
14.8
15.2
15.6
16.0
16.4
16.8
17.3
17.7
Time

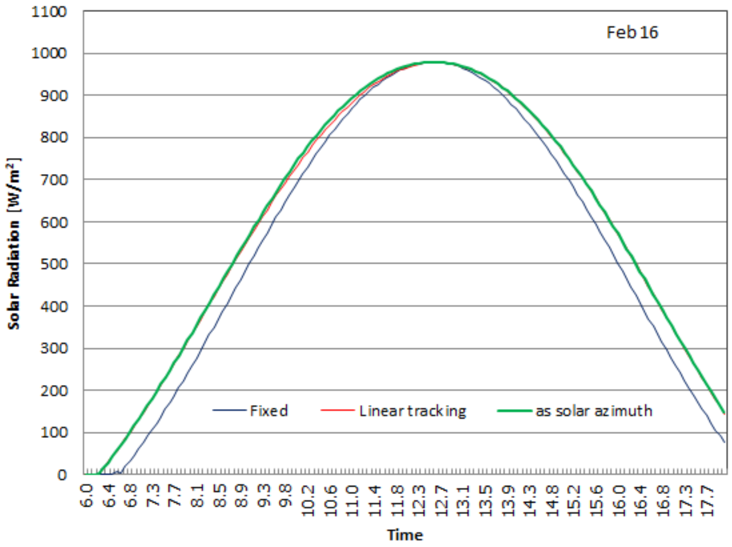
Feb 16
Solar Radiation [W/m²]
0
100
200
300
400
500
600
700
800
900
1000
1100
Fixed
Linear tracking
as solar azimuth
6.0
6.4
6.8
7.3
7.7
8.1
8.5
8.9
9.3
9.8
10.2
10.6
11.0
11.4
11.8
12.3
12.7
13.1
13.5
13.9
14.3
14.8
15.2
15.6
16.0
16.4
16.8
17.3
17.7
Time

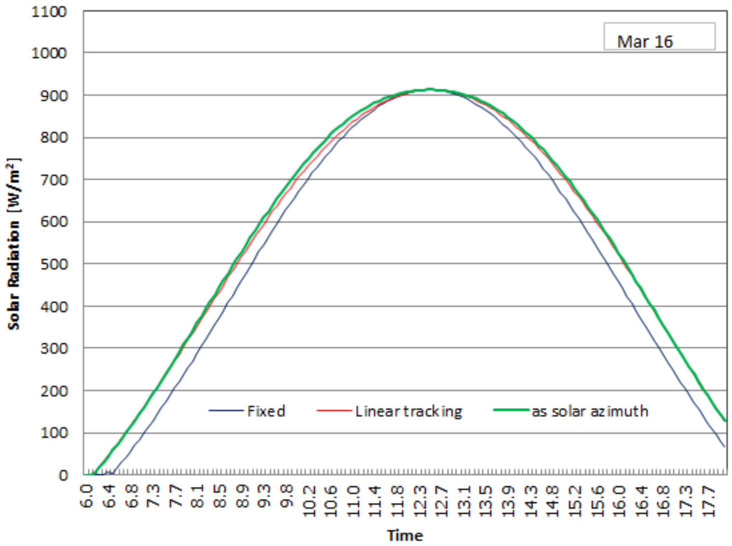
Mar 16
Solar Radiation [W/m²]
0
100
200
300
400
500
600
700
800
900
1000
1100
Fixed
Linear tracking
as solar azimuth
6.0
6.4
6.8
7.3
7.7
8.1
8.5
8.9
9.3
9.8
10.2
10.6
11.0
11.4
11.8
12.3
12.7
13.1
13.5
13.9
14.3
14.8
15.2
15.6
16.0
16.4
16.8
17.3
17.7
Time

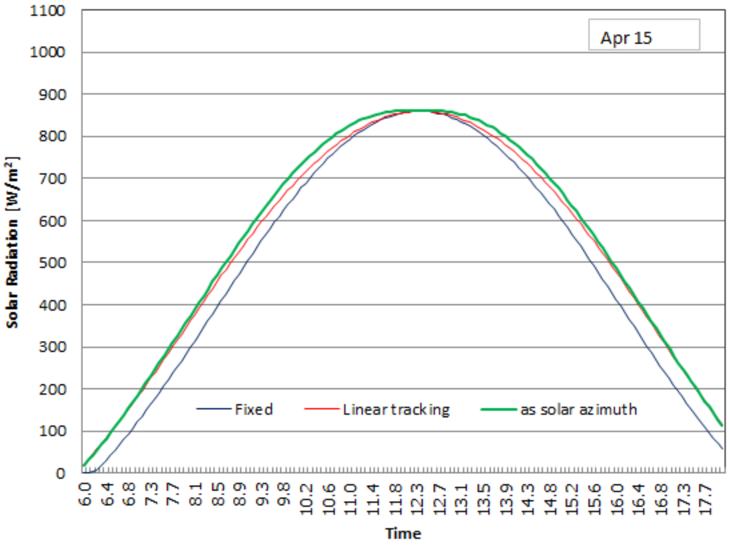
Apr 15
Solar Radiation [W/m²]
0
100
200
300
400
500
600
700
800
900
1000
1100
Fixed
Linear tracking
as solar azimuth
6.0
6.4
6.8
7.3
7.7
8.1
8.5
8.9
9.3
9.8
10.2
10.6
11.0
11.4
11.8
12.3
12.7
13.1
13.5
13.9
14.3
14.8
15.2
15.6
16.0
16.4
16.8
17.3
17.7
Time

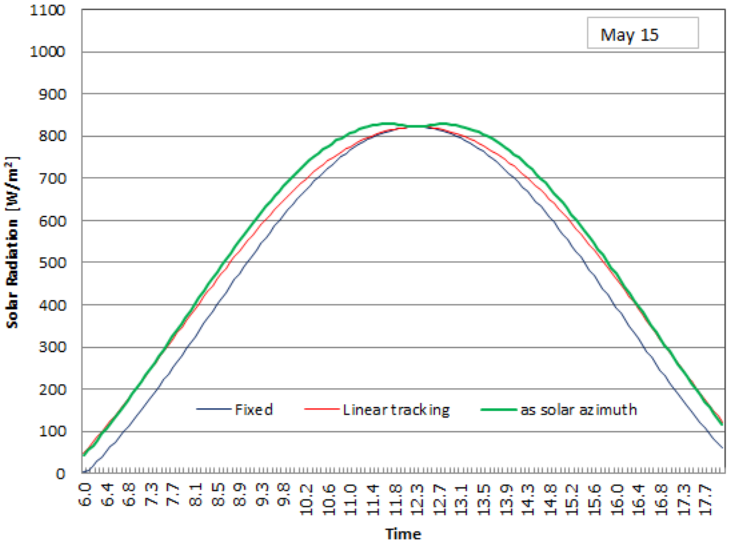
May 15
Solar Radiation [W/m²]
0
100
200
300
400
500
600
700
800
900
1000
1100
Fixed
Linear tracking
as solar azimuth
6.0
6.4
6.8
7.3
7.7
8.1
8.5
8.9
9.3
9.8
10.2
10.6
11.0
11.4
11.8
12.3
12.7
13.1
13.5
13.9
14.3
14.8
15.2
15.6
16.0
16.4
16.8
17.3
17.7
Time

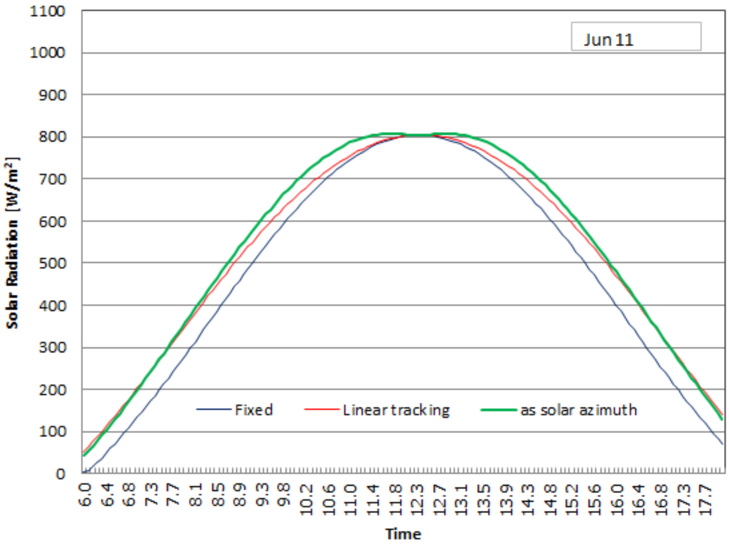
Jun 11
Solar Radiation [W/m²]
0
100
200
300
400
500
600
700
800
900
1000
1100
Fixed
Linear tracking
as solar azimuth
6.0
6.4
6.8
7.3
7.7
8.1
8.5
8.9
9.3
9.8
10.2
10.6
11.0
11.4
11.8
12.3
12.7
13.1
13.5
13.9
14.3
14.8
15.2
15.6
16.0
16.4
16.8
17.3
17.7
Time

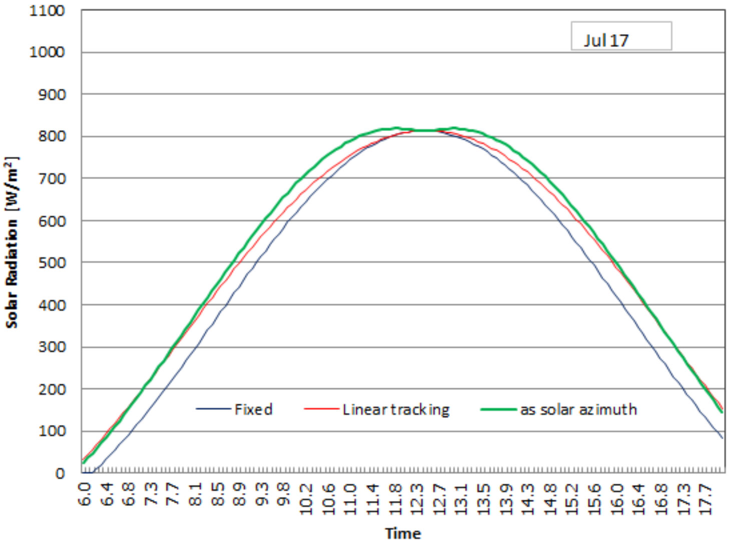
Jul 17
Solar Radiation [W/m²]
1100
1000
900
800
700
600
500
400
300
200
100
0
Fixed
Linear tracking
as solar azimuth
6.0
6.4
6.8
7.3
7.7
8.1
8.5
8.9
9.3
9.8
10.2
10.6
11.0
11.4
11.8
12.3
12.7
13.1
13.5
13.9
14.3
14.8
15.2
15.6
16.0
16.4
16.8
17.3
17.7
Time

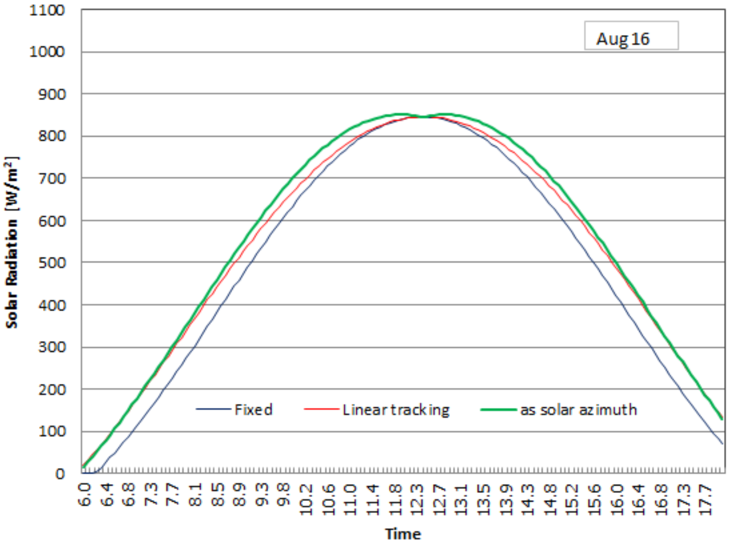
Aug 16
Solar Radiation [W/m²]
1100
1000
900
800
700
600
500
400
300
200
100
0
Fixed
Linear tracking
as solar azimuth
6.0
6.4
6.8
7.3
7.7
8.1
8.5
8.9
9.3
9.8
10.2
10.6
11.0
11.4
11.8
12.3
12.7
13.1
13.5
13.9
14.3
14.8
15.2
15.6
16.0
16.4
16.8
17.3
17.7
Time

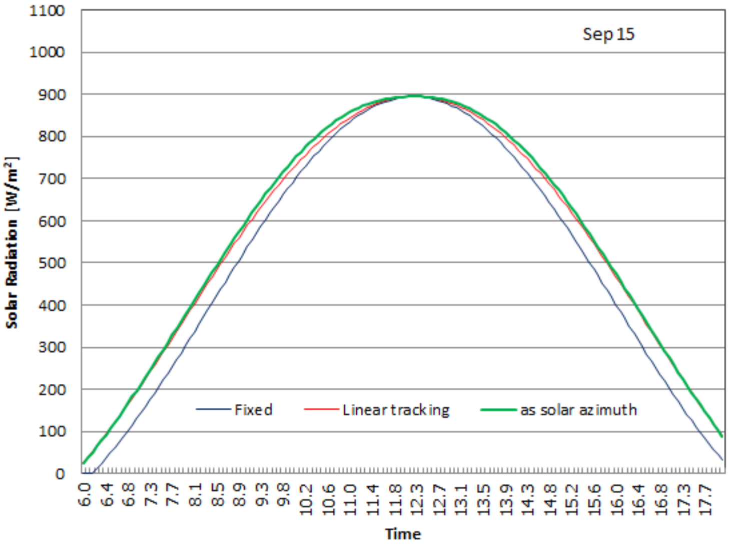
Sep 15
Solar Radiation [W/m²]
1100
1000
900
800
700
600
500
400
300
200
100
0
Fixed
Linear tracking
as solar azimuth
6.0
6.4
6.8
7.3
7.7
8.1
8.5
8.9
9.3
9.8
10.2
10.6
11.0
11.4
11.8
12.3
12.7
13.1
13.5
13.9
14.3
14.8
15.2
15.6
16.0
16.4
16.8
17.3
17.7
Time

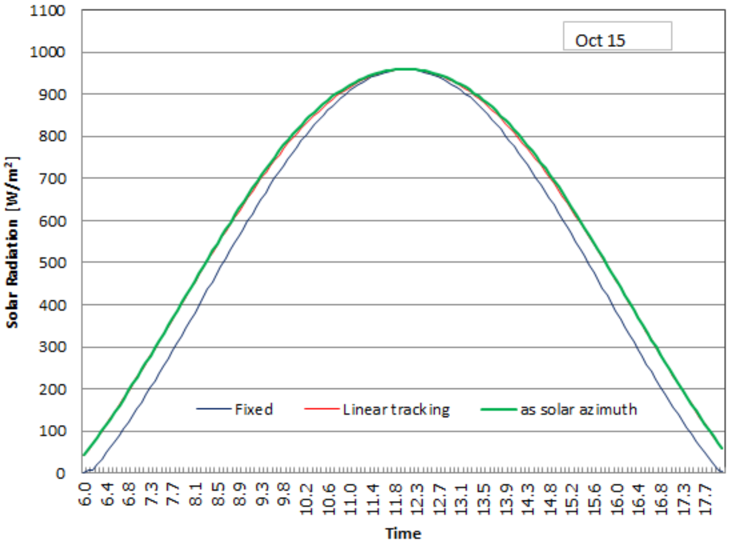
Oct 15
Solar Radiation [W/m²]
1100
1000
900
800
700
600
500
400
300
200
100
0
Fixed
Linear tracking
as solar azimuth
6.0
6.4
6.8
7.3
7.7
8.1
8.5
8.9
9.3
9.8
10.2
10.6
11.0
11.4
11.8
12.3
12.7
13.1
13.5
13.9
14.3
14.8
15.2
15.6
16.0
16.4
16.8
17.3
17.7
Time

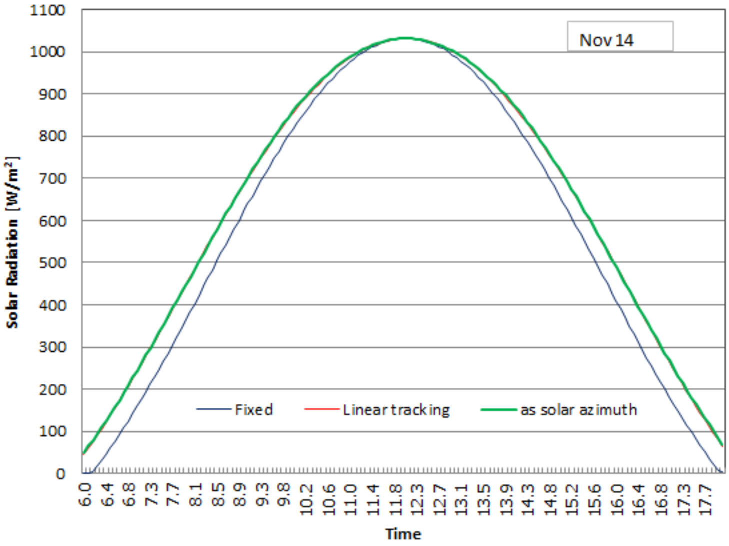
Nov 14
Solar Radiation [W/m²]
1100
1000
900
800
700
600
500
400
300
200
100
0
Fixed
Linear tracking
as solar azimuth
6.0
6.4
6.8
7.3
7.7
8.1
8.5
8.9
9.3
9.8
10.2
10.6
11.0
11.4
11.8
12.3
12.7
13.1
13.5
13.9
14.3
14.8
15.2
15.6
16.0
16.4
16.8
17.3
17.7
Time

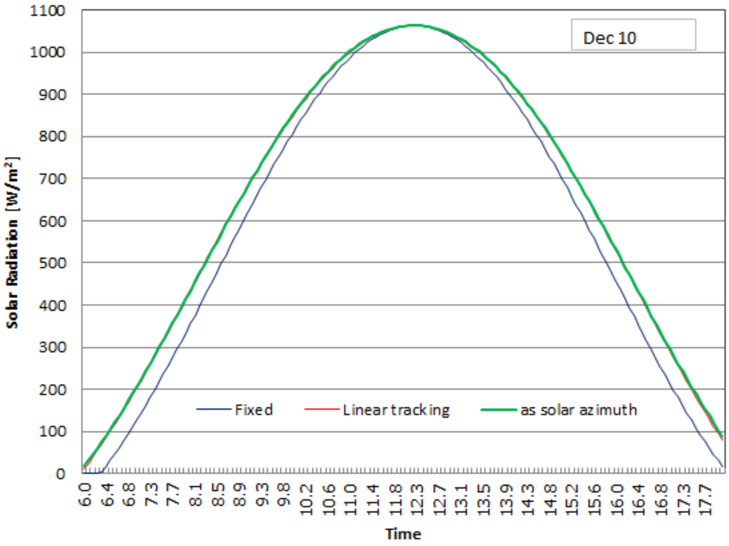
Dec 10
Solar Radiation [W/m²]
1100
1000
900
800
700
600
500
400
300
200
100
0
Fixed
Linear tracking
as solar azimuth
6.0
6.4
6.8
7.3
7.7
8.1
8.5
8.9
9.3
9.8
10.2
10.6
11.0
11.4
11.8
12.3
12.7
13.1
13.5
13.9
14.3
14.8
15.2
15.6
16.0
16.4
16.8
17.3
17.7
Time